DOI: 10.1002/hlca.202000184

FULL PAPER

HELVETICA chimica acta

Phenazine Radical Cations as Efficient Homogeneous and Heterogeneous Catalysts for the Cross-Dehydrogenative Aza-*Henry* Reaction

Felix Unglaube,[a] Paul Hünemörder,[a] Xuewen Guo,[a] Zixu Chen,[b] Dengxu Wang,[b] and Esteban Mejía*[a]

[a] Leibniz Institute for Catalysis, Albert-Einstein-Str. 29a, DE-18059 Rostock, Germany,
e-mail: Esteban.Mejia@Catalysis.de
[b] Key Laboratory of Special Functional Aggregated Materials, Ministry of Education, School of Chemistry and Chemical Engineering, Shandong University, Jinan 250100, P. R. China

Dedicated to Prof. *Antonio Togni* on the occasion of his 65th birthday

The redox activity of molecular phenazine catalysts has been previously exploited for aerobic oxidative amine homo- and cross-coupling reactions. In this contribution, we have extended the reaction scope of this novel type of organocatalyst and used them in the cross-dehydrogenative aza-*Henry* coupling of isoquinolines with nitromethane under aerobic conditions. Additionally, we have designed and prepared a novel porous organic polymer by cross-linking of tetrakis(4-bromophenyl)silane and dihydrophenazine through Pd-catalyzed *Buchwald-Hartwig* cross-coupling. This new type of heterogeneous catalyst, apart from being robust and easily reusable, also showed outstanding catalytic activities and improved selectivity compared to its molecular counterpart. A plausible reaction mechanism was proposed based on spectroscopic and kinetic measurements.

Keywords: aerobic oxidation, aza-*Henry* reaction, cross-coupling, cross-dehydrogenative coupling, phenazines, polymers, porous organic polymers.

Introduction

The development of metal-free catalysts has been the focus of many research efforts during the last decades, due to the environmental[1–4] and toxicologic[5] concerns associated with the widespread use of noble metal-based catalysts and the increasing urge towards sustainable chemical processes.[6–14] Among the many alternatives, carbon-based materials have attracted great interest not only due to their low cost, but also thanks to their robustness and recyclability (making them ideal candidates for industrial applications), along with the tunability of their surface physicochemical properties.[15–21] These materials have been used as catalysts in several organic reactions including oxidations and reductions,[22–25] *Friedel-Crafts* alkylations,[26] and hydrocarbon dehydrogenations.[27]

The catalytic activity of heterogeneous organocatalysts depends on two main factors, the porosity (since a high surface area and pore volume enhances substrate adsorption and transport),[15–21,28] and the presence of active sites (which can adsorb/coordinate and activate the reactants and stabilize reaction intermediates). A common approach to obtain such sites at the catalyst surface is the doping with heteroatoms, specially nitrogen,[29–39] either by chemical modification of a pre-existing material, or by calcination of pre-organized precursors such as organic polymers,[40] metal-organic frameworks (MOFs),[41] and covalently linked porous polymers (CPP).[42] The latter material class, also known as (micro)porous organic polymers (POPs or MOPs) or covalent organic

Supporting information for this article is available on the WWW under https://doi.org/10.1002/hlca.202000184

frameworks (COFs), have gained a lot of attention on their own right, due to their tunable properties and their myriad of potential applications,[43–45] including gas capture and separation,[46–51] and catalysis.[52–55] The synthesis of these modular materials has been achieved through cross-linking of functional building blocks using different methodologies including *Friedel-Crafts* arylation,[42,56,57] *Suzuki*,[58] *Sonogashira*,[59] and *Buchwald-Hartwig* cross-couplings,[60] and *Yamamoto* polymerization,[61] among others.

Recently, our group reported a novel synthetic methodology for the synthesis of the elusive 1,4-functional tetramethylpyrazines (*Scheme 1,A*) and used them as catalysts for the aerobic oxidative homocoupling of primary amines, thanks to the reversible redox behavior of these compounds and the remarkable stability of their radical-cationic form.[62] We explored further the exploitation of stable radical cations as oxidation catalysts with the development of a series of 5,10-disubstitued phenazines (*Scheme 1,B*) which showed remarkable activities for the oxidative homo and cross coupling of amines.[63] Interestingly, even though the strong redox properties of phenazines and the stability of their open-shell derivatives are relatively well-known, there are very few additional reports on their use as redox catalysts. Notable examples are the reports from the *Miyake* group on their use as catalysts for photoinduced atom transfer radical polymerization,[64,65] and the use the non-functionalized 5,10-dihydrophenazine (in stoichiometric amounts) as oxidant and proton-transfer reagent for aldehyde esterification.[53] Inspired by our previous works on the preparation of hybrid porous polymers based on polyhedral oligomeric silsesquioxane (POSS),[42] and the aforementioned pyrazine and phenazine radical-cation oxidation catalysts,[63] we designed and synthesized a novel type of covalently linked porous polymers exhibiting tetrakis(phenyl) silane moieties as structural elements cross-linked by phenazine groups (*Scheme 1,C*).

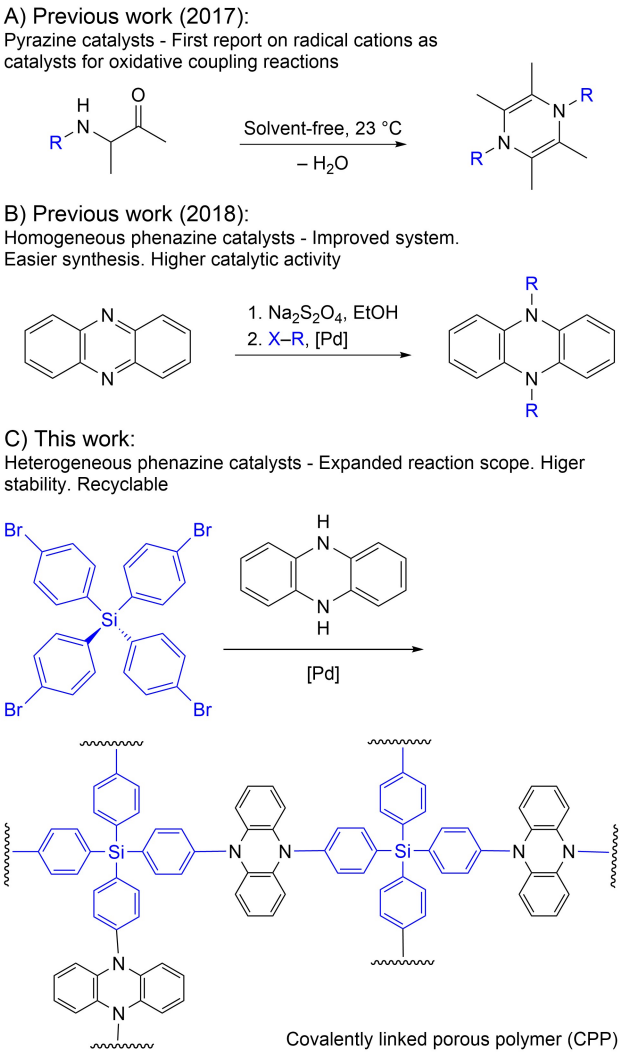

Scheme 1. Development of metal-free radical cation precursors to be used as catalysts in aerobic oxidative coupling reactions.

Moreover, we extended the reaction scope of this type of catalysts and used successfully both the molecular derivatives (**1a**–**1f**) and the CCP (**2**) for C–C bond formations through cross-dehydrogenative aza-*Henry* reactions. This represents, to the best of our knowledge, the first example of a metal-free heterogeneous system for cross-dehydrogenative coupling reactions.

During the preparation of this manuscript, a similar type of microporous polymer containing phenazine groups was independently reported by *Guo* and co-workers, which showed remarkable activity on the oxidative coupling of amines.[66]

Results and Discussion

Catalyst Synthesis and Characterization

Homogenous phenazine pre-catalyst (**1a**–**1f**) were prepared according to the reported procedure.[63] The active 7-π-electron radical-cationic state of the phenazines was achieved by oxidation with stoichiometric amounts of $NOBF_4$ (*Scheme 2*).[63]

The covalently linked porous polymer (CPP) containing immobilized phenazine moieties (**2**) was prepared by cross-linking of tetrakis(4-bromophenyl)silane and dihydrophenazine through Pd-catalyzed *Buchwald-Hartwig* cross-coupling in toluene at 110 °C for

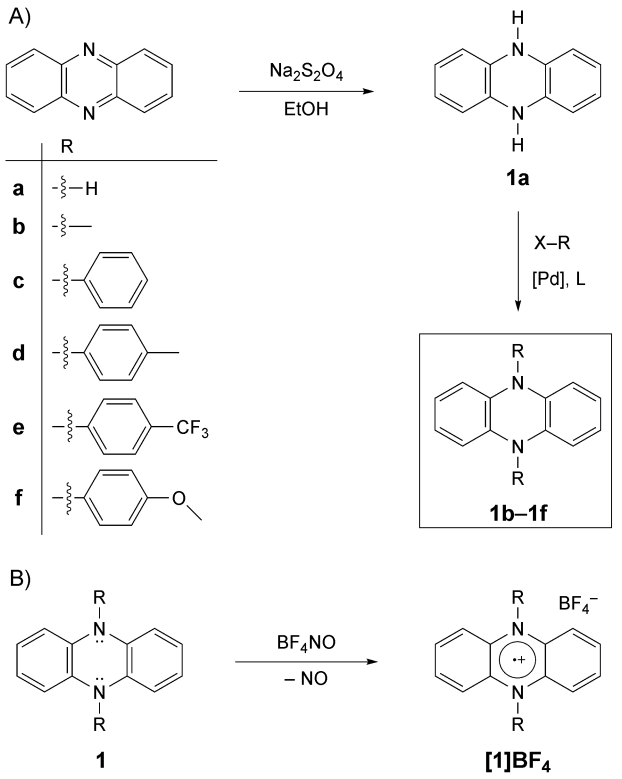

Scheme 2. A) General synthesis of the molecular phenazine pre-catalysts. B) Preparation of the catalytic active species through oxidation.

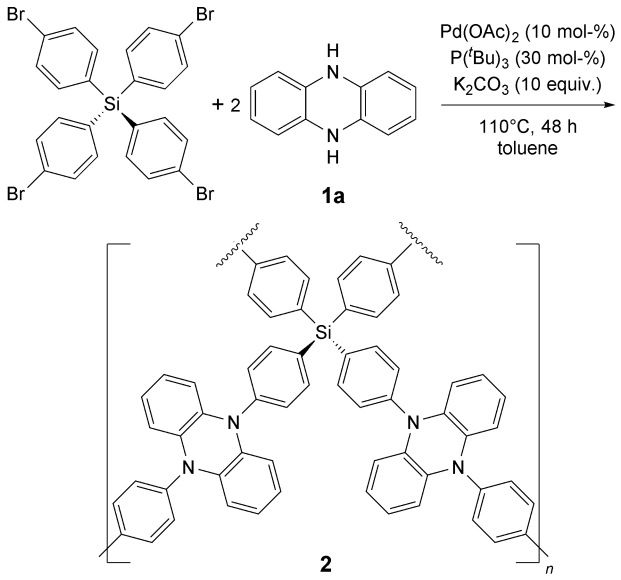

Scheme 3. Synthesis of covalently linked porous polymer (CPP) containing immobilized phenazine moieties (**2**) through *Buchwald-Hartwig* cross-coupling.

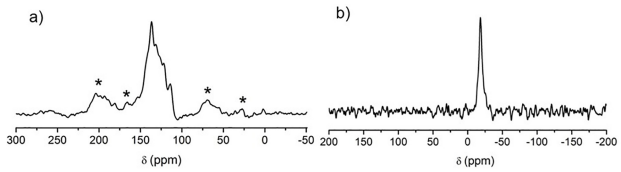

Figure 1. Solid-state ^{13}C-NMR (a) and ^{29}Si-NMR (b) spectra of **2**. The signals with the asterisks are attributed to the spinning side bands.

48 h (*Scheme 3*). After the cross-linking, the crude product was recovered by filtration, washed, and extracted with several solvents, and dried under vacuum to yield the final material. The received red powder is insoluble in common solvents, such as water, methanol, chloroform, THF, and acetone, thereby indicating their high cross-linking degree of the network.

To confirm its structure, the CPP **2** was fully characterized by solid-state ^{13}C, ^{29}Si Cross Polarization/Magic Angle Spinning Nuclear Magnetic Resonance (CP/MAS NMR) and *Fourier*-transform infrared spectroscopy (FTIR). In the solid-state ^{13}C-NMR spectrum (*Figure 1,a*), the peaks ranging from 105 to 150 ppm are attributed to the sp^2 phenylene carbon atoms from the silicon-centered unit and phenazine unit. In the ^{29}Si-NMR spectrum (*Figure 1,b*), one signal at −18 ppm was observed and can be attributed to the central Si atom in the framework (the chemical shift of the starting material was −13.52 in $CDCl_3$),[67] indicating no occurrence of Si–C cleavage during the polymerization.

The porosity of catalyst **2** was investigated by nitrogen adsorption-desorption experiment at 77 K. The material gives rise to a combination of type I and IV isotherms (*Figure 2,a*),[68] which exhibits a sharp uptake at low relative pressures and then a gradually increasing uptake at higher relative pressures with a hysteresis. The *Brunauer-Emmett–Teller* (BET) surface area (S_{BET}) and the total pore volume (V_{total}) of the catalyst are 377 $m^2 g^{-1}$ and 0.27 $cm^3 g^{-1}$. The micropore surface area (S_{micro}) and the micropore volume (V_{micro}) were calculated to be 253 $m^2 g^{-1}$ and 0.10 $cm^3 g^{-1}$ by using the t-plot method. Thus, the V_{micro}/V_{total} ratio, representing the contribution of microporosity in the network, is 0.37, suggesting that the network is predominantly mesoporous. The pore size distribution (PSD) was evaluated by nonlocal density functional theory (NL-DFT). The material possesses a relatively uniform micropores with an average diameter centered at *ca.* 1.23 nm and a broad

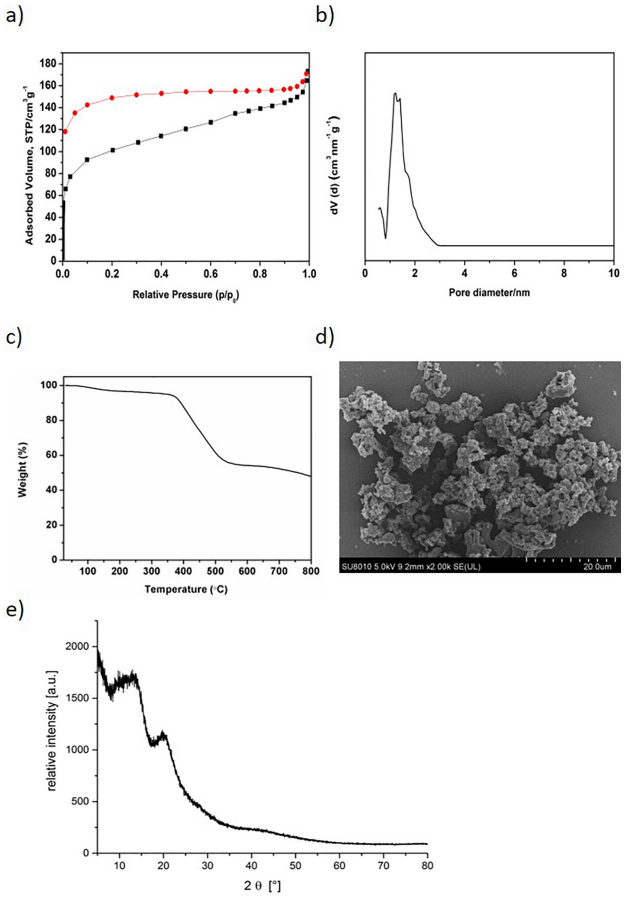

Figure 2. Solid state characterization of **2**. a) Nitrogen adsorption-desorption isotherm. b) Pore size distribution curve. c) TGA curves under N_2 atmosphere with a heating rate of 10 °C min^{-1}. d) FE-SEM image. e) Powder XRD pattern.

mesopore (*Figure 2,b*). Thermogravimetric analysis (TGA) reveals that the catalyst shows high thermal stability with T_d (5% mass loss) at approximately 350 °C, comparable to other silicon-centered porous materials (*Figure 2,c*).[42] Field emission scanning electron microscopy (FE-SEM) of **2** shows that the solid consists of a nanostructured interlinking irregular particles of lamellar shape (*Figure 2,d*). In contrast to the conventional amorphous porous polymers, the X-ray diffraction (XRD) pattern of **2** shows two broad reflexes centered at 12.7° and 19.4°, equivalent to d-spacing distances of 6.2 and 4.4 Å, respectively (*Figure 2,e*). This finding indicates that the obtained CPP have locally molecular homogeneity and long-range order although the degree of the order is not very high. Indeed, those crystalline or partially crystalline porous organic polymers are very rare, to the best of our knowledge only one example from 2010 is reported in literature.[69]

The presence of unpaired electrons at the material's surface was assessed by electron paramagnetic resonance (EPR), just as it was previously investigated for its molecular counterparts.[63] A very strong signal was observed at 3524 Gs (*g* value of 2.003), which is in the typical range for an organic radical (*Figure 3*).[70,71] Importantly, this strong signal was observed both in the solid sample and in suspension in methyl tert-butyl ether (MTBE) and was not affected by bubbling of oxygen in the sample (*Figure 3*). This important observation suggests that **2**, as prepared, already possess open-shell phenazine moieties, without additional oxidative treatment. It can be thus assumed that **2** was readily oxidized by atmospheric oxygen during its work-up. In contrast to what was observed for molecular phenazines (measured and simulated in a previous work),[63] no hyperfine splitting was observed. Only marginal shoulders are visible and do not lead to structural information about the radical. The broad signals suggest that the radical moieties in the catalyst are relatively close to each other, resulting in an interaction of the paramagnetic moments.

In the FTIR spectroscopy of **2** (*Figure 4*, upper trace), the characteristic Si–C stretching vibration was observed at 1481 cm^{-1}. Compared to the vibration spectrum of dihydrophenazine (**1a**, *Figure 4*, lower trace) The disappearance of absorption band (N–H stretching) at *ca.* 3501 cm^{-1}, confirms the successful cross-coupling between the tetraphenylsilane monomer and **1a**. Parts of the infrared vibrations of **1a** can also be found in the IR spectrum of **2**, *e.g.* the bands at 1481, 1387, 1261, 1038, 912, 762, 735 and 679 cm^{-1},

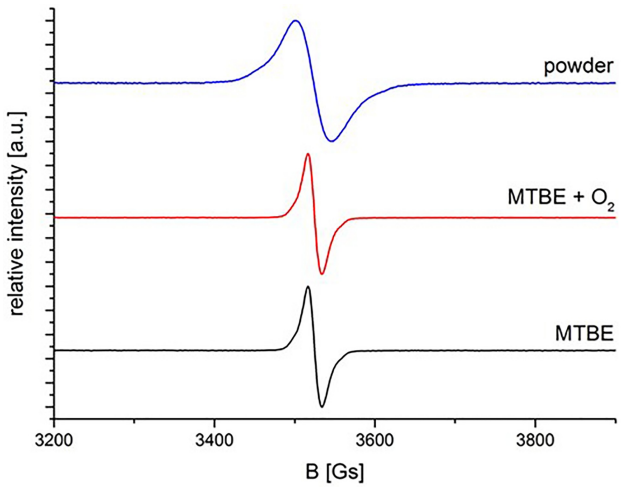

Figure 3. Normalized EPR signals from pure **2** (powder), **2** in solution in MTB with oxygen (MTBE + O_2), and **2** in MTBE under inert atmosphere (MTBE).

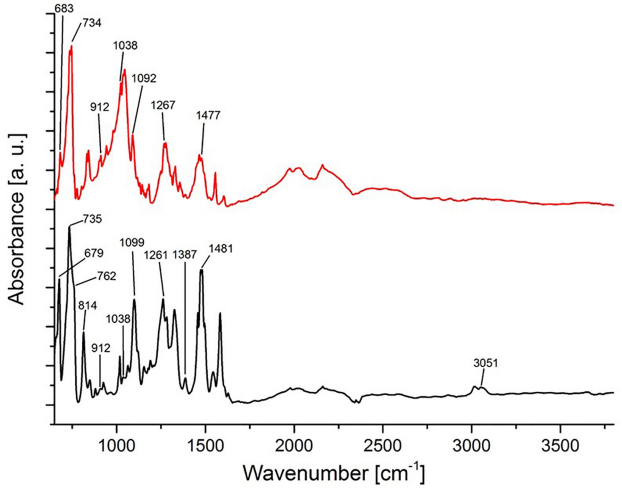

Figure 4. IR Spectra of pure **2** as powder (upper trace) and **1a** dissolved in dichloromethane (lower trace).

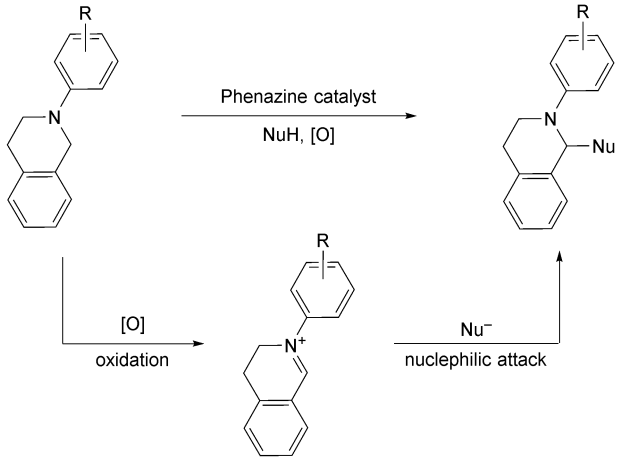

Scheme 4. Generation and reactivity of hydroisoquinoline-2-ium intermediates in a cross-dehydrogenative coupling reaction.

which can be attributed to the phenyl moieties of the phenazine molecule. Other bands such as those at 3064, 3051 and 3014 cm^{-1} as well as 1099 cm^{-1} can be associated with the increased number of phenyl rings in the polymer and to Si–Ph vibrations, respectively (see also *Figure S6*).

Catalytic Experiments

The ability of phenazine radical cations to furnish iminium ions from amines through single-electron transfer (SET) under aerobic conditions has been previously observed and confirmed in our previous investigations.[63] Thus, we figured, it should be possible to trap different carbon nucleophiles with these reactive intermediates under the proper conditions (*Scheme 4*), just as it has been thoroughly exploited in cross-dehydrogenative couplings (CDC),[72] a powerful and elegant methodology for furnishing C–C bonds from two different C–H groups.[73–75]

Hence, we selected the cross-dehydrogenative aza-*Henry* (nitro-*Mannich*) reaction between hydroisoquinolines and nitromethane as model system to test our hypothesis. This reaction has been widely used in organic synthesis since the introduced nitro synthon can be converted into 1,2-diamines[76,77] or α-aminocarbonyls (*Nef* reaction).[78] There are many catalytic approaches to achieve this transformation, mostly using noble metals like Ru,[79] and Ir,[80] and more recently under photochemical conditions using metal complexes.[81,82] Metal-free photocatalytic systems, which often use Eosin as photosensitizer,[83] are relatively rare.[84] Beside the catalytic systems there is a larger number of reports using stoichiometric amounts of oxidants like DDQ,[85] or H_2O_2.[86] However, metal-free systems able to catalyze aza-*Henry* reactions under thermal conditions are still under-developed, displaying very slow kinetics or requiring stoichiometric amounts of additives which leads to significant amounts of waste.[87–89]

Thus, initial experiments on the cross-dehydrogenative aza-*Henry* reaction using the preactivated molecular phenazine radical cations ([**1**]BF_4 and the heterogeneous counterpart **2**) as catalysts, hydroisoquinoline **3a** as pre-electrophile and nitromethane as both pre-nucleophile and solvent, were performed under atmospheric oxygen pressure at elevated temperature (*Table 1*). The possible formation of the 3,4-dihydroisoquinolone side product **5a** will not be addressed at this point; the chemoselectivity of this reaction is described further below (*Table 2*).

To ensure that any detected catalytic activity is solely caused by the catalysts, inductively coupled plasma/optical emission spectrometry (ICP-OES) analysis was performed to **3a** to assess the presence of traces of copper coming from the substrate synthesis, (since copper itself is well able to catalyze the reaction).[90] No copper was detected by this method, so if there are any traces of this metal, should be in amounts lower than 0.005 mol-% (relative to **3a**). However, since there is a small product being formed in the absence of phenazine catalyst (*Table 1*, *entry 8*), we performed the reaction with the addition of 1 mol-% CuI to the mixture, leading to a only slightly

Table 1. Aerobic cross-dehydrogenative aza-*Henry* reaction catalyzed by molecular phenazine radical cations.

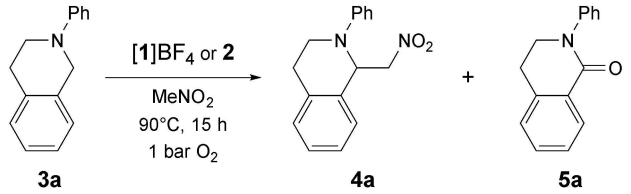

Entry[a]	Catalyst	**3a** consumption [%][b]
1	**1a**	3
2	**1b**	90
3	**1c**	43
4	**1d**	51
5	**1e**	40
6	**1f**	56
7	**2**	80
8	–	15
9[c]	CuI	21
10[d]	**1b**	26

[a] Reaction conditions (if not stated differently): 90 °C, 1 bar oxygen, neat, 15 h, 5 mol-% of catalyst [**1**]BF_4 or 20 mg/$mmol_{subs}$ of catalyst **2**. [b] Determined by GC/MS. [c] 1 mol-% of CuI. [d] Using air as oxidant.

Table 2. Substrate conversion with different catalysts applied to the reaction.

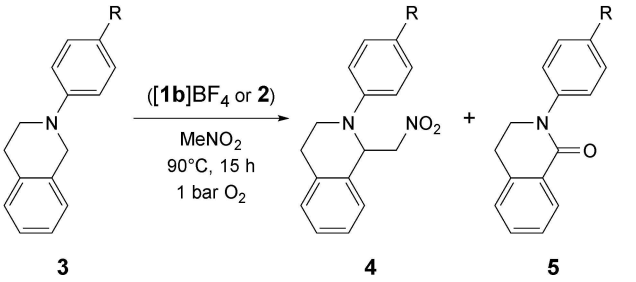

Entry[a]	Substrate (R)	Catalyst	Yield of **4** [%][b]	Yield of **5** [%][b]
1	**3a** (H)	**1b**	73	25
2		**2**	78	0
3	**3b** (CH_3)	**1b**	19	80
4		**2**	81	24
5	**3c** (OCH_3)	**1b**	4	95
6		**2**	55	21
7	**3d** (CF_3)	**1b**	75	21
8		**2**	99	0

[a] Reaction conditions: 90 °C, 1 bar oxygen, 15 h, 5 mol-% of catalyst [**1b**]BF_4 or 20 mg/$mmol_{subs}$ of catalyst **2**. [b] Determined by GC.

increased conversion compared to the reaction without any catalyst (*Table 1*, *entry 10*). Consequently, the catalytic activity can be attributed to the phenazine catalysts **1**.

The conditions were optimized to improve the reaction yield. The loading of the catalyst **1** was varied from 0.1 to 50 mol-% relative to the substrate **3a** (*Figure S7*). The lowest loading (0.1 mol-%) showed no effect on the reaction, while it reached a maximum of 86% with 5 mol-% catalyst loading and dropped rapidly with higher loadings. Therefore, 5 mol-% was chosen as catalyst loading for all further experiments with **1**. Loadings higher than 20 mol-% showed no catalytic effect, suggesting that the catalyst is deactivated through intramolecular interactions between catalyst molecules. The reversible dimerization of the curved π-radical cations, as described by *Hiroto* and *Shinokubo* upon increasing its concentration could explained the observed deactivation.[91] The optimal catalyst loading for the phenazine-containing CPP (**2**) was also investigated, varying it from 5 to 25 mg per mmol of substrate ($mmol_{subs}$). The yield increased with rising catalyst loading form 25% up to a plateau at 78% when 20 mg/$mmol_{subs}$ were used (*Figure S8*).

A temperature screening was also performed, for which catalyst **1b** was selected (*Figure S9*). It was observed that the conversion of **3a** is possible at room temperature (20% yield), while the yield increased continuously until 90 °C, where it reached a plateau at around 90% yield. Therefore, 90 °C was chosen as reaction temperature for the rest of the experiments. A solvent screening was not conducted since nitromethane serves as both substrate and solvent. The influence of a decreased oxygen partial pressure was investigated by using air instead of pure oxygen as oxidation agent, resulting in a considerable drop in the catalyst activity *Table 1*, *entry 10*).

In line with our previous observations,[63] pre-oxidation of the homogeneous phenazine catalysts with $NOBF_4$ was necessary to achieve reproducible catalytic activity, hence for this investigation also the homogeneous catalysts were used as the corresponding BF_4 salt ([**1**]BF_4). Interestingly, in contrast to its molecular analogues, the heterogeneous catalyst **2** does not require pre-oxidation. Hence previous treatment with either $NOBF_4$, H_2O_2 or O_2 does not lead to any improvement in catalytic activity and was therefore not applied for the subsequent experiments.

All the tested catalyst (except from the underivatized phenazine **1a**, which shows an inhibitory effect, resulting in conversions even lower that the uncatalyzed reaction) showed good to excellent conversions, being **1b** the most active (*Table 1*,

entry 2). The catalytic activity of the **1c** to **1f** increased along with the electron density at the *N*-Phenyl rings (*Table 1*, *entry 3–6*). Their overall lower catalytic activity compared to **1b** can be explained through their lower ionization energy. In our previous work, the ionization energies of these molecules were determined with DFT calculations.[63] For instance, the lower ionization barrier for radical formation of **1f** (129.8 kcal mol^{-1}) compared to **1b** (139.9 kcal mol^{-1}) suggests a more stable radical state and therefore, lower reactivity under catalytic conditions.

To our delight, the newly synthesized covalently linked porous polymer **2** displayed a good catalytic activity under these conditions (80 %, *Table 1*, *entry 7*). Moreover, it was possible the recover and re-use the heterogeneous catalyst (up to eight time) with only a small initial apparent activity decrease after which it plateaued at 74 % (*Figure S11*).

A substrate screening was done to investigate the influence of both the electrophile and nucleophile on the reaction yield and selectivity. For this purpose, the molecular pre-catalyst **1b** and the CPP **2** were chosen (*Table 2*).

Apart from the expected aza-*Henry* coupling product (**4**), almost in every case the corresponding 3,4-dihydroisoquinolone (**5**) was obtained, in some cases, to our surprise, as the major product (the identity of the isoquinolone product was confirmed by single crystal X-ray diffractometry; *Figures S3* and *S4*). These amides are common minor side products in oxidation of benzylic amines and isoquinolines and its selective formation can be achieved under the right reaction conditions.[63,92,93] What came as a surprise was the strong selectivity dependence on the electronic properties of the substrate. For instance, when the molecular catalyst [**1b**]BF_4 was used with the electron rich *p*-methoxy tetrahydroisoquinoline **3c**, the almost exclusive formation of the isoquinolone **5c** was achieved (95 %, *Table 2*, *entry 5*). In contrast, using the same catalyst with the electron poor *p*-trifluoromethyl containing substrate **3d**, the desired aza-*Henry* coupling product **4d** is obtained as the major product (75 %, *Table 2*, *entry 7*). Interestingly, when the heterogeneous catalyst **2** was used, the preferred reaction product was always the aza-*Henry* adduct **5**, in approximately 2 : 1 ratio (**4c** to **5c**) with the methoxy-substituted substrate (*Table 2*, *entry 6*). and in quantitative amounts with the trifluoromethylated analogue (*Table 2*, *entry 8*).

Mechanistic Investigations

Kinetic plots for the aza-*Henry* reaction (substrate concentration *vs.* time, *Figures S12–S17*) for substrates bearing different substituents in *para* position of the 2-phenyl group (**3a–3d**) using pre-catalyst **1b** showed a pseudo zero order dependency every case, indicating that the reaction rate is highly limited by the concentration of one reactant, presumably by the diffusion of oxygen, as previously observed in oxidative amine coupling reactions with the same catalysts.[63] Consumption rates (*k*) were obtained from the slope of the linear function of the substrate concentration against time (*Table 3*).

When using the homogeneous catalyst ([**1b**]BF_4), data clearly showed that the stronger the electron donating capability of the substituent in para position of the phenyl ring, the faster the substrate consumption in the reaction was. This trend was further observed in the corresponding *Hammett*-plot (*Figure 5*), attesting the intermediacy of a positively charged species (iminium) that is stabilized by the

Table 3. *Hammett* constants (σ_p) and kinetic constants (*k*) of substrate consumption from **3a–3d** with pre-catalyst **1b**.

Entry[a]	Substrate (R)	σ_p	k [L mol^{-1} s^{-1}]	Lg (k)
1	**3a** (H)	0	−0.028	−1.553
3	**3b** (CH_3)	−0.17	−0.029	−1.524
5	**3c** (OCH_3)	−0.27	−0.034	−1.469
7	**3d** (CF_3)	0.54	−0.021	−1.686

[a] Reaction conditions: 90 °C, 1 bar oxygen, 15 h, 5 mol-% of catalyst [**1b**]BF_4.

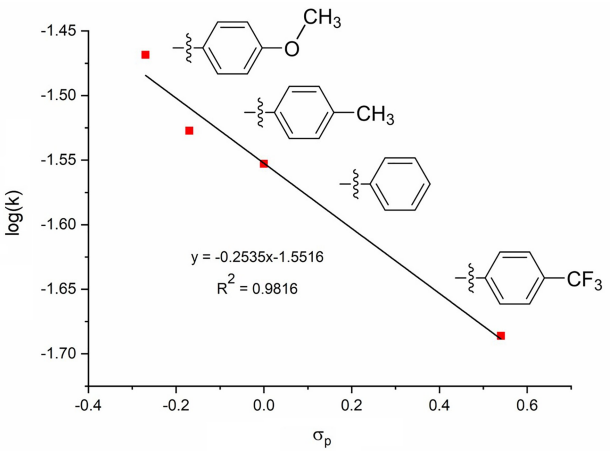

Figure 5. *Hammett* σρ free-energy relationship for the homogeneous cross-dehydrogenative aza-*Henry* coupling of tetrahydroisoquinolines with nitromethane under aerobic conditions.

influence of electron-donating groups.[94] Interestingly, when using catalyst **2**, a clear σρ free-energy relationship was not observed, suggesting that polar interactions do not play any role in the rate determining step in the heterogeneous system.

Based on our previous fluorescence, UV/Vis and EPR analysis of phenazine catalyzed oxidation reactions,[63] together with the kinetic observation described above, a general reaction mechanism can be proposed (*Scheme 5*). In an initial stage, the phenazine pre-catalyst needs to be oxidized. Hence, since the O_2 concentration in the reaction mixture is low, in the case of the molecular catalysts **1**, a better performance is achieved by pre-treatment with $NOBF_4$. Conversely, since CPP **2** already attains its activated radical-cationic stage by reaction with atmospheric oxygen in the solid state (as confirmed by EPR), a pre-oxidation is not necessary and can directly be used in catalysis. Either way, oxidation of **1** shall produce the corresponding phenazine radical-cation and, when oxygen enters the cycle, a reduced oxygen species, most likely a superoxide radical anion, $O_2^{\bullet-}$ (alas, an undisputable proof of its intermediacy remains elusive). Subsequently, SET with the isoquinoline substrate **3** regenerates the closed-shell phenazine **1** and yields the amine radical cation **6**. After the formation of **6**, hydrogen atom abstraction by $O_2^{\bullet-}$ forms radical **7** and the hydroperoxyl radical HOO•. These two species might subsequently react either by direct recombination or SET to produce an equilibrating mixture of the iminium ion **8** and hydroperoxide **9**.[95–97] The intermediacy of the positively charged species **8** is supported by the observed *Hammett* relationships (see above). The iminium intermediate **8** can thus undergo two different pathways: it reacts electrophilically with nitromethane to generate the expected aza-*Henry* adduct **4** or it is nucleophilic attacked by adventitious water in the solution to produce a hemiaminal (**10**), which can be oxidized to form the isoquinolone product (**5**).[92,93] Addition of molecular sieves to the mixture inhibited the formation of **5**, thus confirming this hypothesis.

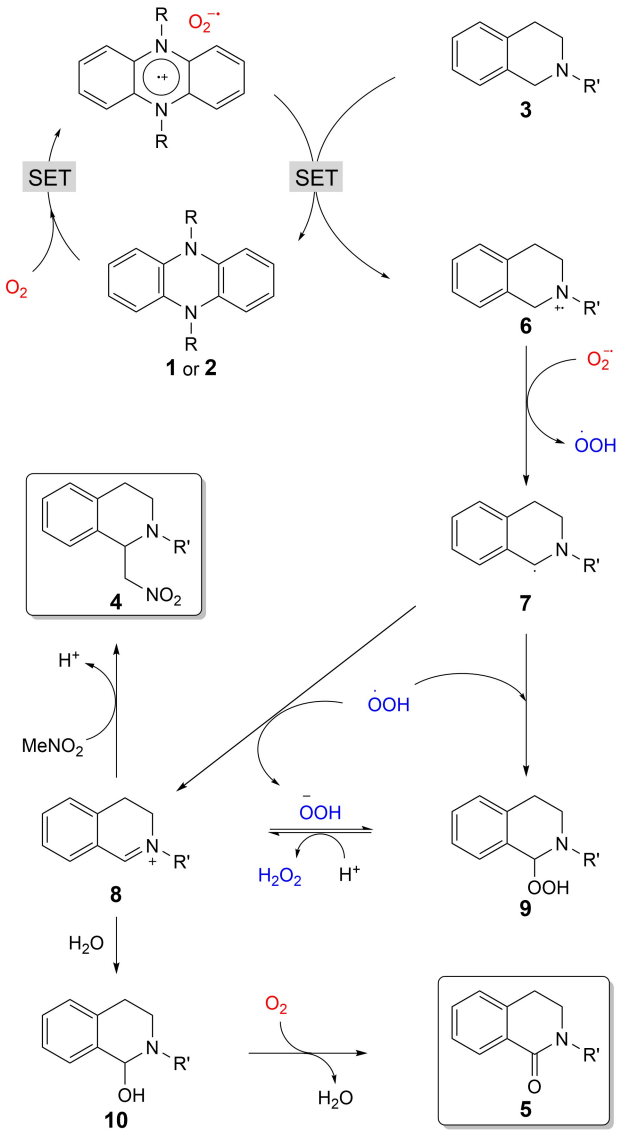

Scheme 5. Proposed reaction mechanism for phenazine catalyzed cross-dehydrogenative aza-*Henry* reaction in the presence of atmospheric oxygen.

We hypothesize that in the homogeneous system the nucleophilic attack to the cationic intermediate **6** is the slower step, thus allowing the side reaction with water and leading to the (sometimes preferential) formation of **5**. On the contrary, for the heterogeneous system, since the iminium intermediate is not involved in the rate determining step, its rapid coupling with nitromethane impairs is collateral reaction with water and results in the preferential formation of the aza-*Henry* product **4**. Moreover, mass-transport effects at the surface of the heterogeneous catalysts might play an important role on the reaction selectivity, but further mechanistic investigations are necessary to assess this possibility.

Conclusions

Molecular phenazine catalysts have previously shown outstanding activities as catalysts for aerobic oxidative amine coupling and cross-coupling reactions. In this contribution we expanded the reaction scope of this novel type of metal-free oxidation catalyst and dem-

onstrated their applicability in cross-dehydrogenative aza-*Henry* coupling of different isoquinolines with nitromethane under aerobic conditions. Moreover, we have designed and synthesized a porous covalent polymer containing catalytically active phenazine moieties cross-linked by tetraphenylsilane moieties. This novel porous material was fully characterized, and its catalytic potential was demonstrated in the aza-*Henry* coupling reaction. Interestingly, the selectivity of the reaction towards the expected aza-*Henry* product (*vs.* the corresponding isoquinolone) depends heavily on the electronic situation of the substrate and on the nature of the catalyst. Thus, with the heterogeneous polymeric phenazine catalysts **2**, the aza-*Henry* product (**4**) was obtained preferentially, disregarding the electronic properties of the substrate. A plausible reaction mechanism was proposed, considering previous spectroscopic observations along with additional kinetic experiments. Importantly, these organocatalysts are among the few that can catalyze aza-*Henry* reactions under thermal conditions. Moreover, CPP **2** is, to best of our knowledge, the first metal-free heterogeneous system reported for cross-dehydrogenative coupling reactions.

Experimental Section

General Information

All reactions were performed under *Schlenk*, air/moisture-free conditions. All solvents were dried, degassed and stored in septum-sealed flasks over molecular sieves under Ar atmosphere. Solvents for catalyst preparation were distilled over Na, CaH_2 or molecular sieves following standardized procedures. All chemicals were purchased from commercial sources (unless stated otherwise). Most of chemicals were used without further purification. The purity of purchased products was confirmed by either NMR spectroscopy or GC/MS analysis.

NMR Spectra in liquid phase were recorded in $CDCl_3$ or (D_8)Toluene using *Bruker Avance 300* spectrometer with *QNP* probe head (^{1}H: 300 MHz, ^{13}C: 75 MHz) or *Bruker Avance 400* spectrometer (^{1}H: 400 MHz, ^{13}C: 100 MHz). The calibration of the spectra was carried out on referenced with residual solvent shifts and were reported as parts per million [ppm] relative to $SiMe_4$. Multiplicities are abbreviated as follows: *singlet* (*s*), *doublet* (*d*), *triplet* (*t*), *quartet* (*q*), *doublet-doublet* (*dd*), *doublet-triplet* (*dt*), *quintet* (*quint*), *sextet* (*sext*), *septet* (*sept*), *multiplet* (*m*), and broad (br.). Samples were generally measured at room temperature (297 K). Deuterated solvents were degassed and distilled if necessary.

Solid-state ^{13}C cross-polarization/magic-angle-spinning (CP/MAS) NMR and ^{29}Si-MAS-NMR data were collected on *Bruker AVANCE-500* NMR Spectrometer operating at a magnetic field strength of 9.4 T. The resonance frequencies at this field strength were 125 and 99 MHz for ^{13}C-NMR and ^{29}Si-NMR, respectively. A *Chemagnetics* 5 mm triple-resonance MAS probe was used to acquire ^{13}C- and ^{29}Si-NMR spectra. ^{29}Si-MAS-NMR spectrum with high power proton decoupling was recorded using a $\pi/2$ pulse length of 5 μs, a recycle delay of 120 s and a spinning rate of 5 kHz.

ESI-TOF spectra were obtained on *Waters Q-TOF* micro mass spectrometer. The samples were dissolved in MeOH/H_2O (9:1) mixture with 0.1% HCOOH to achieve sufficient ionization. All chromatograms were obtained on GC analysis was performed on *Hewlett-Packard 6890* Series. Samples were dissolved in tetrahydrofuran (THF) and sampled into the GC column. GC/MS analysis was performed on A*gilent 6890/5973* GC/MS or on *Agilent 7890/5977* GC/MS. Samples were dissolved in tetrahydrofuran (THF).

IR Spectra were recorded on a *Nicolet Avatar 370* (*Thermo Electron*) FT-IR spectrometer equipped with a smart endurance *ATR* accessory.

Thermogravimetric analysis (TGA) was performed under N_2 using a *TA SDTQ600* at a temperature range of room temperature to 800 °C with a heating rate of 10 °C min^{-1}. To eliminate the effect of possible adsorption of moisture from atmosphere, all the samples were dried at 100 °C under vacuum for 10 h before measurements.

Field-emission scanning electron microscopy (FE-SEM) experiment was performed by using *HITACHI S4800* Spectrometer.

The EPR spectra were recorded at 300 K with a *Bruker EMX CW*-micro spectrometer equipped with an *ER 4119HS-WI* high-sensitivity optical resonator. *g* Values have been calculated from the resonance field B0 and the resonance frequency ν using the resonance condition $h\nu = g\beta B0$.

The molecular phenazine catalysts (**1a**–**1f**) and their corresponding tetrafluoroborate salts ([**1**]BF_4)

were obtained following the previously reported procedures.[63]

Synthesis of Covalent Porous Polymer **2**

A three-necked flask was charged with tetrakis(4-bromophenyl)silane (1.96 g, 3 mmol), palladium(II) acetate (68.39 mg, 0.3 mmol), potassium carbonate (4.19 g, 30.36 mmol) and tri-*tert*-butylphosphine (226.6 mg, 1.12 mmol) in toluene (40 mL) under Ar atmosphere. The resultant mixture was bubbled with Ar under stirring for at least 0.5 h at room temperature and then dihydrophenazine (1.09 g, 6 mmol) was added. Then the mixture was stirred at 110 °C for 48 h. After the reaction, the precipitate was filtered, washed with THF, chloroform, water, methanol, and acetone to remove unconsumed monomers, inorganic salts, catalyst and other residues. Further purification was carried out by *Soxhlet* extraction with THF for 24 h and chloroform for 24 h. Finally, the product was dried in a vacuum at 80 °C to obtain a brown solid with the yield of 91 %. Anal. calc. for $C_{48}H_2N_4Si$: C 83.24, H 4.62, N 8.08; found: C 78.14, H 5.01, N 7.95.

Substrate Synthesis

Dihydroisoquinoline derivatives (**3a**–**3d**) were prepared according to the reported procedure,[98] given exemplarily for 2-phenyl-1,2-dihydroisoquinoline **3a**. All substrates were synthesized following the *General Procedure*.

2-Phenyl-1,2-dihydroisoquinoline (**3a**), *General Procedure*. Copper(I) iodide (0.213 g, 1 mmol) and potassium phosphate (4.25 g, 20 mmol) were added into a 50 ml three-neck round-bottom flask with a *Dimroth* condenser, a *Schlenk* valve and a *Teflon*® magnetic stirrer. The flask was evacuated tree times for 20 min and flushed with Ar. Subsequently, 2-propanol (10 ml), ethylene glycol (1.2 ml, 20 mmol), 1,2,3,4-tetrahydroisoquinoline (2 ml, 15 mmol) and iodobenzene (1.12 ml, 10 mmol) were added successively with a syringe at room temperature. The resulting orange mixture was heated at 90 °C in an oil bath and stirred at this temperature for 24 h. After cooling to room temperature, 20 mL water was added, and the organic layer was extracted tree times with 20 ml diethyl ether. The combined organic phases were washed with brine (100 g sodium chloride per 1 L water) in a separating funnel. The solution was dried over magnesium sulfate and filtrated. Silica was added to the organic phase and the diethyl ether was removed by rotary evaporation. After performing thin layer chromatography (TLC) the product was purified by column chromatography over silica gel (heptane/ethyl acetate 10 : 1). The desired product was collected with an R_f value of 0.7. The desired product was a white solid, mass 1.6 g (yield: 51 %). The obtained spectra match literature reports:[99,100] ^{1}H-NMR (300 MHz, $CDCl_3$): 7.28–7.19 (*m*, 2 H); 7.16–7.07 (*m*, 4 H); 6.97–6.89 (*m*, 2 H); 6.81–6.73 (*m*, 1 H); 4.35 (*s*, 2 H); 3.51 (*t*, J = 5.9, 2 H); 2.93 (*t*, J = 5.7, 2 H). ^{13}C-NMR (75 MHz, $CDCl_3$): 150.69; 135.02; 134.61; 129.34; 128.66; 126.68; 126.46; 126.16; 118.79; 115.28; 50.87; 46.66; 29.26; 27.07.

2-(4-Methylphenyl)-1,2,3,4-tetrahydroisoquinoline (**3b**). Following the *General Procedure*, copper(I) iodide (0.203 g, 1 mmol), potassium phosphate (4.26 g, 20 mmol) and 1-iodo-4-methylbenzene (2.18 g, 10 mmol) were added together with 2-propanol (10 mL), ethylene glycol (1.2 mL, 20 mmol), 1,2,3,4-tetrahydroisoquinoline (2 mL, 15 mmol). The pure product was obtained by column chromatography over silica gel using a mixture of pentane and ethyl acetate (10 : 1), R_f 0.6. The desired product was a yellowish oil, mass 2.5 g (yield 75 %). The obtained spectra match literature reports:[100] ^{1}H-NMR (400 MHz, $CDCl_3$): 7.66–7.60 (*m*, 1 H); 7.29–7.19 (*m*, 2 H); 4.43 (*s*, 1 H); 3.58 (*t*, J = 5.9, 1 H); 3.05 (*t*, J = 5.7, 1 H); 2.38 (*s*, 1 H). ^{13}C-NMR (101 MHz, $CDCl_3$): 148.63; 137.22; 131.21; 129.73; 128.60; 126.55; 126.26; 125.95; 115.83; 51.44; 47.25; 29.14; 21.04.

2-(4-Methoxyphenyl)-1,2,3,4-tetrahydroisoquinoline (**3c**). Following the *General Procedure*, copper(I) iodide (0.203 g, 1 mmol), potassium phosphate (4.27 g, 20 mmol) and 1-iodo-4-methoxybenzene(2.34 g, 10 mmol) were added together with 2-propanol (10 mL), ethylene glycol (1.2 mL, 20 mmol), 1,2,3,4-tetrahydroisoquinoline (2 mL, 15 mmol). The pure product was obtained by column chromatography over silica gel using a mixture of pentane and ethyl acetate (10 : 1), R_f 0.8. The desired product was a white solid, mass 2.4 g (yield: 68 %). Single crystals of **3c** were obtained by slow evaporation of a saturated diethyl ether solution at room temperature. The obtained spectra match literature reports:[100] ^{1}H-NMR (400 MHz, $CDCl_3$): 7.21–7.10 (*m*, 1 H); 7.02–6.97 (*m*, 1 H); 6.90–6.85 (*m*, 1 H); 4.31 (*s*, 1 H); 3.79 (*s*, 1 H); 3.46 (*t*, J = 5.9, 1 H); 6.91–6.85 (*m*, 1 H); 7.59–7.53 (*m*, 1 H); 3.00 (*t*, J = 5.9 1 H); 7.02–6.96 (*m*, 1 H). ^{13}C-NMR (101 MHz, $CDCl_3$): 153.61; 145.48; 138.32; 128.82;

126.64; 126.03; 118.15; 116.48; 55.77; 55.44; 52.80; 29.24.

2-[4-(Trifluoromethyl)phenyl]-1,2,3,4-tetrahydroisoquinoline (**3d**). Following the *General Procedure*, copper(I) iodide (0.230 g, 1 mmol), potassium phosphate (4.26 g, 20 mmol) and 1-Iodo-4-(trifluoromethyl)benzene (2.72 g, 10 mmol) were added together with 2-propanol (10 mL), ethylene glycol (1.2 mL, 20 mmol), 1,2,3,4-tetrahydroisoquinoline (2 mL, 15 mmol). The pure product was obtained by column chromatography over silica gel using a mixture of pentane and ethyl acetate (10:1), R_f 0.4. The desired product was a white solid, mass 3.5 g (yield: 83%). Single crystals of **3d** were obtained by slow evaporation of a saturated diethyl ether solution at room temperature. The obtained spectra match literature reports:[100] ^{1}H-NMR (300 MHz, $CDCl_3$): 7.53 (*d*, *J* = 8.6 1 H); 7.27–7.15 (*m*, 2 H); 6.95 (*d*, *J* = 8.7 2 H); 4.50 (*s*, 1 H); 3.64 (*t*, *J* = 5.9, 2 H); 3.01 (*t*, *J* = 5.9, 3 H). ^{13}C-NMR (75 MHz, $CDCl_3$): 152.27; 138.17; 135.05; 133.95; 128.47; 126.84; 126.65; 126.48; 113.07; 77.58; 77.16; 76.74; 49.56; 45.35; 32.04; 29.11; 22.85; 14.26. ^{19}F-NMR (282 MHz, $CDCl_3$): −61.03.

Catalysis

The *General Procedure* for the catalytic aza-*Henry* reaction is given exemplarily for the 1-(nitromethyl)-2-phenyl-1,2,3,4-tetrahydroisoquinoline **4a**. The other products were synthesized following the *General Procedure*.

1-(Nitromethyl)-2-phenyl-1,2,3,4-tetrahydroisoquinoline (**4a**), *General Procedure*. 2-Phenyl-1,2-dihydroisoquinoline (0.95 mmol, 200 mg), 0.048 mmol of catalyst [**1**][BF_4^-] (5 mol-%) or 20 mg of 5,10-di(4-methoxyphenyl)-5,10-dihydrophenazine **2** and nitromethane (37 mmol, 0.5 ml, 39 eq) were added together in a *Schlenk* flask. The solution was flushed tree times with oxygen. A balloon with oxygen (*ca.* 1 bar) was attached to the *Schlenk* valve. The reaction was conducted for 15 h at 90 °C in an oil bath. After performing TLC with the cold mixture, the product was purified by column chromatography over silica gel (heptane/ethyl acetate 10:1). The product was collected with an R_f value of 0.8. The desired product was a greenish liquid. For yields, see *Table 2*. The obtained spectra match literature reports:[101] ^{1}H-NMR (300 MHz, $CDCl_3$): 7.29–7.11 (*m*, 6 H); 6.99 (*d*, *J* = 8.3, 2 H); 6.86 (*t*, *J* = 7.2, 1 H); 5.56 (*t*, *J* = 7.2, 1 H); 4.88 (*dd*, *J* = 11.8, 7.8, 1 H); 4.57 (*dd*, *J* = 11.8, 6.6, 1 H); 3.73–3.54 (*m*, 2 H); 3.16–2.98 (*m*, 1 H); 2.80 (*dt*, *J* = 16.3, 4.8, 1 H). ^{13}C-NMR (75 MHz, $CDCl_3$): 148.57; 135.42; 133.08; 129.65; 129.33; 128.27; 127.15; 126.85; 119.59; 115.26; 78.94; 58.34; 42.24; 26.62. ESI-TOF: 268.12057 ($C_{16}H_{16}O_2N_2^+$, [*M* + H]$^+$; calc. 268.12063). The side product 2-phenyl-3,4-dihydroisoquinolin-1(2*H*)-one (**5a**) was analyzed through GC/MS. The EI-MS spectrum matches literature reports[102] (see *Supporting Information*). Single crystals of **5a** were obtained by slow evaporation of a saturated diethyl ether solution at room temperature. Then, one single crystal was removed from the mother liquor and used as seed in a fresh diethyl ether solution and allow to grow for 14 days at room temperature. The molecular structure of **5a** was confirmed by single-crystal X-ray diffraction (see *Supporting Information*).

2-(4-Methylphenyl)-1-(nitromethyl)-1,2,3,4-tetrahydroisoquinoline (**4b**). Following the *General Procedure*, using 2-(4-methylphenyl)-1,2,3,4-tetrahydroisoquinoline (200 mg, 0.9 mmol). The pure product was obtained by column chromatography over silica gel using a mixture of pentane and ethyl acetate (10:1), R_f 0.8. The desired product was a yellowish liquid. For yields, see *Table 2*. The product was analyzed by GC/MS and EI-MS. The EI-MS spectrum is given in the supporting Information. The obtained NMR spectra match literature reports:[101] ^{1}H-NMR (300 MHz, $CDCl_3$): 7.19–7.03 (*m*, 2 H); 7.02–6.97 (*m*, 1 H); 6.84–6.78 (*m*, 1 H); 5.42 (*t*, *J* = 8.0, 6.4, 1 H); 4.78 (*dd*, *J* = 11.9, 8.0, 1 H); 4.49 (*dd*, *J* = 11.8, 6.4, 1 H); 3.62–3.46 (*m*, 1 H); 2.99 (*ddd*, *J* = 15.4, 9.0, 6.0, 1 H); 2.69 (*dt*, *J* = 16.4, 4.6, 1 H); 2.26 (*s*, 3 H). The side product 2-(4-methylphenyl)-3,4-dihydroisoquinolin-1(2*H*)-one (**5b**) was analyzed through GC/MS (see *Supporting Information*).

2-(4-Methoxyphenyl)-1-(nitromethyl)-1,2,3,4-tetrahydroisoquinoline (**4c**). Following the *General Procedure*, using 2-(4-methoxyphenyl)-1,2,3,4-tetrahydroisoquinoline (200 mg, 0.9 mmol). The pure product was obtained by column chromatography over silica gel using a mixture of pentane and ethyl acetate (10:1), R_f 0.8. The desired product was a yellowish liquid. For yields, see *Table 2*. The obtained spectra match literature reports:[101] ^{1}H-NMR (400 MHz, CD_3CN): 7.27–7.20 (*m*, 3 H); 7.18–7.14 (*m*, 1 H); 6.95–6.89 (*m*, 2 H); 6.83–6.78 (*m*, 2 H); 5.41 (*dd*, *J* = 9.6, 5.3, 1 H); 4.89 (*dd*, *J* = 12.4, 9.6, 1 H); 4.73 (*dd*, *J* = 12.4, 5.2, 1 H); 3.70 (*s*, 3 H); 3.62–3.52 (*m*, 2 H); 2.94–2.84 (*m*, 1 H); 2.64 (*m*, 1 H). ^{13}C-NMR (101 MHz, CD_3CN): 154.77; 144.21; 136.78; 133.72; 130.40; 128.66; 128.29; 127.26; 119.71; 118.34; 115.49; 115.45; 79.64; 59.19; 56.03; 43.27; 25.74; 1.94;

1.73; 1.52; 1.47; 1.32; 1.26; 1.11; 0.91; 0.70. The side product 2-(4-methoxyphenyl)-3,4-dihydroisoquinolin-1(2*H*)-one (**5c**) was analyzed through GC/MS (see *Supporting Information*).

1-(Nitromethyl)-2-[4-(trifluoromethyl)phenyl]-1,2,3,4-tetrahydroisoquinoline (**4d**). Following the *General Procedure* using 2-[4-(trifluoromethyl)phenyl]-1,2,3,4-tetrahydroisoquinoline (200 mg, 0.9 mmol). The pure product was obtained by column chromatography over silica gel using a mixture of pentane and ethyl acetate (10:1), R_f 0.8. The product was a yellowish liquid. For yields, see *Table 2*. The obtained spectra match literature reports:[103] ^{1}H-NMR (400 MHz, $CDCl_3$): 7.57 (*m*, 2 H); 7.37–7.25 (*m*, 3 H); 7.20 (*dd*, *J* = 7.5, 1.5, 1 H); 7.07 (*m*, 2 H); 5.68 (*t*, *J* = 7.2, 1 H); 4.92 (*dd*, *J* = 12.0, 7.7, 1 H); 4.65 (*dd*, *J* = 12.0, 6.7, 1 H); 3.78–3.68 (*m*, 2 H); 3.17 (*ddd*, *J* = 16.4, 7.6, 5.7, 1 H); 2.92 (*dt*, *J* = 16.3, 5.4, 1 H). ^{13}C-NMR (101 MHz, $CDCl_3$): 150.61; 134.99; 132.44; 129.28; 128.59; 127.10; 127.04; 126.94; 126.90; 113.41; 78.50; 77.48; 77.16; 76.84; 57.86; 41.84; 26.62. ^{19}F-NMR (282 MHz, $CDCl_3$): −61.36. The side product 2-[4-(trifluoromethyl)phenyl]-3,4-dihydroisoquinolin-1(2*H*)-one (**5d**) was analyzed through GC/MS (see *Supporting Information*).

Supplementary Material

Supporting information for this article is available on the WWW under https://doi.org/10.1002/hlca.202000184. X-Ray crystallographic CIF data were deposited in the *Cambridge Crystallographic Data Centre* and they are available free of charge with the numbers CCDC 1938159 (**3d**), CCDC 1952847 (**3c**) and CCDC 1952651 (**5a**).

Acknowledgements

We would like to warmly thank Dr. *Anke Spannenberg* for the X-Ray diffraction measurements, Dr. *Nils Rockstroh* for the IR spectra and Dr. *Dirk Hollmann* for his support with the EPR experiments. Prof. *Udo Kragl* is also gratefully acknowledged for his constant support. Open access funding enabled and organized by Projekt DEAL.

Author Contribution Statement

F. U., *P. H.* and *X. G.* prepared the molecular catalysts and conducted all the catalytic experiments. *Z. C.* and *D. W.* carried out the synthesis and characterization of the polymeric catalyst. *E. M.* conceived the project and supervised the research. *F. U.*, *D. W.* and *E. M.* wrote the manuscript.

References

[1] M. Saurat, S. Bringezu, 'Platinum Group Metal Flows of Europe, Part 1: Global Supply, Use in Industry, and Shifting of Environmental Impacts', *J. Ind. Ecol.* **2008**, *12*, 754–767.
[2] M. Saurat, S. Bringezu, 'Platinum Group Metal Flows of Europe, Part II: Exploring the Technological and Institutional Potential for Reducing Environmental Impacts', *J. Ind. Ecol.* **2009**, *13*, 406–421.
[3] S. J. Fallon, J. C. White, M. T. McCulloch, '*Porites* corals as recorders of mining and environmental impacts: Misima Island, Papua New Guinea', *Geochim. Cosmochim. Acta* **2002**, *66*, 45–62.
[4] T. Norgate, N. Haque, 'Energy and greenhouse gas impacts of mining and mineral processing operations', *J. Cleaner Prod.* **2010**, *18*, 266–274.
[5] K. S. Egorova, V. P. Ananikov, 'Which Metals are Green for Catalysis? Comparison of the Toxicities of Ni, Cu, Fe, Pd, Pt, Rh, and Au Salts', *Angew. Chem. Int. Ed.* **2016**, *55*, 12150–12162.
[6] D. S. Su, J. Zhang, B. Frank, A. Thomas, X. C. Wang, J. Paraknowitsch, R. Schlögl, 'Metal-Free Heterogeneous Catalysis for Sustainable Chemistry', *ChemSusChem* **2010**, *3*, 169–180.
[7] S. Ahmad, E. Guillén, L. Kavan, M. Grätzel, M. K. Nazeeruddin, 'Metal free sensitizer and catalyst for dye sensitized solar cells', *Energy Environ. Sci.* **2013**, *6*, 3439–3466.
[8] M. Fèvre, J. Pinaud, Y. Gnanou, J. Vignolle, D. Taton, '*N*-Heterocyclic carbenes (NHCs) as organocatalysts and structural components in metal-free polymer synthesis', *Chem. Soc. Rev.* **2013**, *42*, 2142–2172.
[9] S. Wertz, A. Studer, 'Nitroxide-catalyzed transition-metal-free aerobic oxidation processes', *Green Chem.* **2013**, *15*, 3116–3134.
[10] X. Zou, Y. Zhang, 'Noble metal-free hydrogen evolution catalysts for water splitting', *Chem. Soc. Rev.* **2015**, *44*, 5148–5180.
[11] Y. Nie, L. Li, Z. Wei, 'Recent advancements in Pt and Pt-free catalysts for oxygen reduction reaction', *Chem. Soc. Rev.* **2015**, *44*, 2168–2201.
[12] M. Shao, Q. Chang, J.-P. Dodelet, R. Chenitz, 'Recent Advances in Electrocatalysts for Oxygen Reduction Reaction', *Chem. Rev.* **2016**, *116*, 3594–3657.
[13] Y. Xu, M. Kraft, R. Xu, 'Metal-free carbonaceous electrocatalysts and photocatalysts for water splitting', *Chem. Soc. Rev.* **2016**, *45*, 3039–3052.
[14] M. Zhou, H.-L. Wang, S. Guo, 'Towards high-efficiency nanoelectrocatalysts for oxygen reduction through engi-

neering advanced carbon nanomaterials', *Chem. Soc. Rev.* **2016**, *45*, 1273–1307.
[15] C. Huang, C. Li, G. Shi, 'Graphene based catalysts', *Energy Environ. Sci.* **2012**, *5*, 8848–8868.
[16] D. S. Su, S. Perathoner, G. Centi, 'Nanocarbons for the Development of Advanced Catalysts', *Chem. Rev.* **2013**, *113*, 5782–5816.
[17] S. Navalon, A. Dhakshinamoorthy, M. Alvaro, H. Garcia, 'Carbocatalysis by Graphene-Based Materials', *Chem. Rev.* **2014**, *114*, 6179–6212.
[18] P. Tang, G. Hu, M. Li, D. Ma, 'Graphene-Based Metal-Free Catalysts for Catalytic Reactions in the Liquid Phase', *ACS Catal.* **2016**, *6*, 6948–6958.
[19] D. S. Su, G. Wen, S. Wu, F. Peng, R. Schlögl, 'Carbocatalysts in Liquid Phase Reactions', *Angew. Chem. Int. Ed.* **2016**, *56*, 936–964.
[20] X. Liu, L. Dai, 'Carbon-based metal-free catalysts', *Nat. Rev. Mater.* **2016**, *1*, 16064.
[21] X. Fan, G. Zhang, F. Zhang, 'Multiple roles of graphene in heterogeneous catalysis', *Chem. Soc. Rev.* **2015**, *44*, 3023–3035.
[22] B. Chen, L. Wang, S. Gao, 'Recent Advances in Aerobic Oxidation of Alcohols and Amines to Imines', *ACS Catal.* **2015**, *5*, 5851–5876.
[23] Y. Lin, B. Li, Z. Feng, Y. A. Kim, M. Endo, D. S. Su, 'Efficient Metal-Free Catalytic Reaction Pathway for Selective Oxidation of Substituted Phenols', *ACS Catal.* **2015**, *5*, 5921–5926.
[24] J. Qin, S. Wang, H. Ren, Y. Hou, X. Wang, 'Photocatalytic reduction of CO_2 by graphitic carbon nitride polymers derived from urea and barbituric acid', *Appl. Catal. B* **2015**, *179*, 1–8.
[25] S. Yang, L. Peng, P. Huang, X. Wang, Y. Sun, C. Cao, W. Song, 'Nitrogen, Phosphorus, and Sulfur Co–Doped Hollow Carbon Shell as Superior Metal-Free Catalyst for Selective Oxidation of Aromatic Alkanes', *Angew. Chem. Int. Ed.* **2016**, *55*, 4016–4020.
[26] F. Hu, M. Patel, F. Luo, C. Flach, R. Mendelsohn, E. Garfunkel, H. He, M. Szostak, 'Graphene-Catalyzed Direct Friedel-Crafts Alkylation Reactions: Mechanism, Selectivity, and Synthetic Utility', *J. Am. Chem. Soc.* **2015**, *137*, 14473–14480.
[27] J. Gläsel, J. Diao, Z. Feng, M. Hilgart, T. Wolker, D. S. Su, B. J. M. Etzold, 'Mesoporous and Graphitic Carbide-Derived Carbons as Selective and Stable Catalysts for the Dehydrogenation Reaction', *Chem. Mater.* **2015**, *27*, 5719–5725.
[28] M.-M. Titirici, R. J. White, N. Brun, V. L. Budarin, D. S. Su, F. del Monte, J. H. Clark, M. J. MacLachlan, 'Sustainable carbon materials', *Chem. Soc. Rev.* **2015**, *44*, 250–290.
[29] S. Majeed, J. Zhao, L. Zhang, S. Anjum, Z. Liu, G. Xu, 'Synthesis and electrochemical applications of nitrogen-doped carbon nanomaterials', *Nanotechnol. Rev.* **2013**, *2*, 615–635.
[30] W. Kiciński, M. Szala, M. Bystrzejewski, 'Sulfur-doped porous carbons: Synthesis and applications', *Carbon* **2014**, *68*, 1–32.
[31] X.-K. Kong, C.-L. Chen, Q.-W. Chen, 'Doped graphene for metal-free catalysis', *Chem. Soc. Rev.* **2014**, *43*, 2841–2857.
[32] X. Wang, G. Sun, P. Routh, D.-H. Kim, W. Huang, P. Chen, 'Heteroatom-doped graphene materials: syntheses, properties and applications', *Chem. Soc. Rev.* **2014**, *43*, 7067–7098.
[33] J. Duan, S. Chen, M. Jaroniec, S. Z. Qiao, 'Heteroatom-Doped Graphene-Based Materials for Energy-Relevant Electrocatalytic Processes', *ACS Catal.* **2015**, *5*, 5207–5234.
[34] S. Agnoli, M. Favaro, 'Doping graphene with boron: a review of synthesis methods, physicochemical characterization, and emerging applications', *J. Mater. Chem. A* **2016**, *4*, 5002–5025.
[35] M. A. Patel, F. Luo, M. R. Khoshi, E. Rabie, Q. Zhang, C. R. Flach, R. Mendelsohn, E. Garfunkel, M. Szostak, H. He, 'P-Doped Porous Carbon as Metal Free Catalysts for Selective Aerobic Oxidation with an Unexpected Mechanism', *ACS Nano* **2016**, *10*, 2305–2315.
[36] Y. Gao, G. Hu, J. Zhong, Z. Shi, Y. Zhu, D. S. Su, J. Wang, X. Bao, D. Ma, 'Nitrogen-Doped sp^2-Hybridized Carbon as a Superior Catalyst for Selective Oxidation', *Angew. Chem. Int. Ed.* **2013**, *52*, 2109–2113.
[37] Q. Wei, X. Tong, G. Zhang, J. Qiao, Q. Gong, S. Sun, 'Nitrogen-Doped Carbon Nanotube and Graphene Materials for Oxygen Reduction Reactions', *Catalysts* **2015**, *5*, 1574–1602.
[38] O. Y. Podyacheva, Z. R. Ismagilov, 'Nitrogen-doped carbon nanomaterials: To the mechanism of growth, electrical conductivity and application in catalysis', *Catal. Today* **2015**, *249*, 12–22.
[39] M. Li, F. Xu, H. Li, Y. Wang, 'Nitrogen-doped porous carbon materials: promising catalysts or catalyst supports for heterogeneous hydrogenation and oxidation', *Catal. Sci. Technol.* **2016**, *6*, 3670–3693.
[40] M. Saleh, J. N. Tiwari, K. C. Kemp, M. Yousuf, K. S. Kim, 'Highly Selective and Stable Carbon Dioxide Uptake in Polyindole-Derived Microporous Carbon Materials', *Environ. Sci. Technol.* **2013**, *47*, 5467–5473.
[41] K. Shen, X. Chen, J. Chen, Y. Li, 'Development of MOF-Derived Carbon-Based Nanomaterials for Efficient Catalysis', *ACS Catal.* **2016**, *6*, 5887–5903.
[42] D. Wang, E. Mejía, 'POSS-Based Nitrogen-Doped Hierarchically Porous Carbon as Metal-Free Oxidation Catalyst', *ChemistrySelect* **2017**, *2*, 3381–3387.
[43] N. Chaoui, M. Trunk, R. Dawson, J. Schmidt, A. Thomas, 'Trends and challenges for microporous polymers', *Chem. Soc. Rev.* **2017**, *46*, 3302–3321.
[44] T. L. Church, A. B. Jasso-Salcedo, F. Björnerbäck, N. Hedin, 'Sustainability of microporous polymers and their applications', *Sci. China Chem.* **2017**, *60*, 1033–1055.
[45] Q. Li, S. Razzaque, S. Jin, B. Tan, 'Morphology design of microporous organic polymers and their potential applications: an overview', *Sci. China Chem.* **2017**, *60*, 1056–1066.
[46] M. M. Abdelnaby, N. A. A. Qasem, B. A. Al-Maythalony, K. E. Cordova, O. C. S. Al Hamouz, 'A Microporous Organic Copolymer for Selective CO_2 Capture under Humid Conditions', *ACS Sustainable Chem. Eng.* **2019**, *7*, 13941–13948.
[47] G. Chang, Z. Shang, T. Yu, L. Yang, 'Rational design of a novel indole-based microporous organic polymer: en-

hanced carbon dioxide uptake *via* local dipole–π interactions', *J. Mater. Chem. A* **2016**, *4*, 2517–2523.
[48] W. Li, A. Zhang, H. Gao, M. Chen, A. Liu, H. Bai, L. Li, 'Massive preparation of pitch-based organic microporous polymers for gas storage', *Chem. Commun.* **2016**, *52*, 2780–2783.
[49] H. Lim, M. C. Cha, J. Y. Chang, 'Preparation of Microporous Polymers Based on 1,3,5-Triazine Units Showing High CO_2 Adsorption Capacity', *Macromol. Chem. Phys.* **2012**, *213*, 1385–1390.
[50] Y. Yuan, F. Sun, L. Li, P. Cui, G. Zhu, 'Porous aromatic frameworks with anion-templated pore apertures serving as polymeric sieves', *Nat. Commun.* **2014**, *5*, 4260.
[51] L. Zou, J. Yuan, Y. Yuan, J. Gu, G. Li, L. Zhang, Y. Liu, 'A Zn (II) metal-organic framework constructed by a mixed-ligand strategy for CO_2 capture and gas separation', *CrystEngComm* **2019**, *21*, 3289–3294.
[52] V. R. Battula, H. Singh, S. Kumar, I. Bala, S. K. Pal, K. Kailasam, 'Natural Sunlight Driven Oxidative Homocoupling of Amines by a Truxene-Based Conjugated Microporous Polymer', *ACS Catal.* **2018**, *8*, 6751–6759.
[53] S. Chun, Y. K. Chung, 'Transition-Metal-Free Poly(thiazolium) Iodide/1,8-Diazabicyclo[5.4.0]undec-7-ene/Phenazine-Catalyzed Esterification of Aldehydes with Alcohols', *Org. Lett.* **2017**, *19*, 3787–3790.
[54] Z. Liu, Q. Su, P. Ju, X. Li, G. Li, Q. Wu, B. Yang, 'A hydrophilic covalent organic framework for photocatalytic oxidation of benzylamine in water', *Chem. Commun.* **2020**, *56*, 766–769.
[55] V. M. Suresh, S. Bonakala, H. S. Atreya, S. Balasubramanian, T. K. Maji, 'Amide Functionalized Microporous Organic Polymer (Am-MOP) for Selective CO_2 Sorption and Catalysis', *ACS Appl. Mater. Interfaces* **2014**, *6*, 4630–4637.
[56] X. Yang, L. Tan, L. Xia, C. D. Wood, B. Tan, 'Hierarchical Porous Polystyrene Monoliths from PolyHIPE', *Macromol. Rapid Commun.* **2015**, *36*, 1553–1558.
[57] Q. Yu, D. Tan, T. Huang, T. Zhao, L. Li, 'Preparation of asphalt-based microporous organic polymers catalyzed by heteropoly acids', *Green Chem.* **2018**, *20*, 4746–4751.
[58] L. Chen, Y. Yang, Z. Guo, D. Jiang, 'Highly Efficient Activation of Molecular Oxygen with Nanoporous Metalloporphyrin Frameworks in Heterogeneous Systems', *Adv. Mater.* **2011**, *23*, 3149–3154.
[59] K. Zhang, B. Tieke, F. Vilela, P. J. Skabara, 'Conjugated Microporous Networks on the Basis of 2,3,5,6-Tetraarylated Diketopyrrolo[3,4-*C*]pyrrole', *Macromol. Rapid Commun.* **2011**, *32*, 825–830.
[60] Y. Liao, J. Weber, C. F. J. Faul, 'Conjugated microporous polytriphenylamine networks', *Chem. Commun.* **2014**, *50*, 8002–8005.
[61] J. Schmidt, M. Werner, A. Thomas, 'Conjugated Microporous Polymer Networks via Yamamoto Polymerization', *Macromolecules* **2009**, *42*, 4426–4429.
[62] R. Brišar, D. Hollmann, E. Mejía, 'Pyrazine Radical Cations as a Catalyst for the Aerobic Oxidation of Amines', *Eur. J. Org. Chem.* **2017**, 5391–5398.
[63] R. Brišar, F. Unglaube, D. Hollmann, H. Jiao, E. Mejía, 'Aerobic Oxidative Homo-and Cross-Coupling of Amines Catalyzed by Phenazine Radical Cations', *J. Org. Chem.* **2018**, *83*, 13481–13490.
[64] J. C. Theriot, C.-H. Lim, H. Yang, M. D. Ryan, C. B. Musgrave, G. M. Miyake, 'Organocatalyzed atom transfer radical polymerization driven by visible light', *Science* **2016**, *352*, 1082–1086.
[65] J. P. Cole, C. R. Federico, C.-H. Lim, G. M. Miyake, 'Photoinduced Organocatalyzed Atom Transfer Radical Polymerization Using Low ppm Catalyst Loading', *Macromolecules* **2019**, *52*, 747–754.
[66] J. Lin, Z. Guo, H. Zhan, 'A robust phenazine-containing organic polymer as catalyst for amine oxidative coupling reactions', *J. Catal.* **2020**, *385*, 338–344.
[67] M. Wander, P. J. C. Hausoul, L. A. J. M. Sliedregt, B. J. van Steen, G. van Koten, R. J. M. Klein Gebbink, 'Synthesis of Polyaryl Rigid-Core Carbosilane Dendrimers for Supported Organic Synthesis', *Organometallics* **2009**, *28*, 4406–4415.
[68] S. Lowell, J. E. Shields, in 'Powder Surface Area and Porosity', Springer Netherlands, Dordrecht, 1984, pp. 11–13.
[69] W. Chaikittisilp, A. Sugawara, A. Shimojima, T. Okubo, 'Microporous Hybrid Polymer with a Certain Crystallinity Built from Functionalized Cubic Siloxane Cages as a Singular Building Unit', *Chem. Mater.* **2010**, *22*, 4841–4843.
[70] J. L. Grant, V. J. Kramer, R. Ding, L. D. Kispert, 'Carotenoid cation radicals: electrochemical, optical, and EPR study', *J. Am. Chem. Soc.* **1988**, *110*, 2151–2157.
[71] T. Li, G. Tan, D. Shao, J. Li, Z. Zhang, Y. Song, Y. Sui, S. Chen, Y. Fang, X. Wang, 'Magnetic Bistability in a Discrete Organic Radical', *J. Am. Chem. Soc.* **2016**, *138*, 10092–10095.
[72] A. A. Almasalma, E. Mejía, 'Mechanistic Pathways Toward the Synthesis of Heterocycles Under Cross-Dehydrogenative Conditions', in 'Heterocycles via Cross Dehydrogenative Coupling: Synthesis and Functionalization', Eds. A. Srivastava, C. K. Jana, Springer Singapore, Singapore, 2019, pp. 329–356.
[73] C.-J. Li, 'Cross-Dehydrogenative Coupling (CDC): Exploring C–C Bond Formations beyond Functional Group Transformations', *Acc. Chem. Res.* **2009**, *42*, 335–344.
[74] C. Zhang, C. Tang, N. Jiao, 'Recent advances in copper-catalyzed dehydrogenative functionalization *via* a single electron transfer (SET) process', *Chem. Soc. Rev.* **2012**, *41*, 3464–3484.
[75] S. A. Girard, T. Knauber, C.-J. Li, 'The Cross-Dehydrogenative Coupling of C_{sp3}–H Bonds: A Versatile Strategy for C–C Bond Formations', *Angew. Chem. Int. Ed.* **2014**, *53*, 74–100.
[76] J. C. Anderson, A. Noble, D. A. Tocher, 'Reductive Nitro-Mannich Route for the Synthesis of 1, 2-Diamine Containing Indolines and Tetrahydroquinolines', *J. Org. Chem.* **2012**, *77*, 6703–6727.
[77] A. Noble, J. C. Anderson, 'Nitro-Mannich Reaction', *Chem. Rev.* **2013**, *113*, 2887–2939.
[78] N. Ono, 'The Nitro Group in Organic Synthesis', Wiley-VCH, New York, 2001.
[79] H. Bartling, A. Eisenhofer, B. König, R. M. Gschwind, 'The Photocatalyzed Aza-Henry Reaction of N-Aryltetrahydroisoquinolines: Comprehensive Mechanism, $H^{\bullet}$-versus H^{+}-Abstraction, and Background Reactions', *J. Am. Chem. Soc.* **2016**, *138*, 11860–11871.

[80] A. W. Gregory, A. Chambers, A. Hawkins, P. Jakubec, D. J. Dixon, 'Iridium-Catalyzed Reductive Nitro-Mannich Cyclization', *Chem. Eur. J.* **2015**, *21*, 111 – 114.

[81] P. Kumar, S. Varma, S. L. Jain, 'A TiO_2 immobilized Ru(II) polyazine complex: a visible-light active photoredox catalyst for oxidative cyanation of tertiary amines', *J. Mater. Chem. A* **2014**, *2*, 4514 – 4519.

[82] C. Li, R. Dickson, N. Rockstroh, J. Rabeah, D. B. Cordes, A. M. Z. Slawin, P. Hünemörder, A. Spannenberg, M. Bühl, E. Mejía, E. Zysman-Colman, P. Kamer, 'Ligand electronic fine-tuning and its repercussion on the photocatalytic activity and mechanistic pathways of the copper-photocatalysed aza-Henry reaction', *Catal. Sci. Technol.* **2020**, *10*, 7745 – 7756.

[83] D. P. K. Hari, B. König, 'Catalyzed Visible Light Oxidative C–C and C–P bond Formation', *Org. Lett.* **2011**, *13*, 3852 – 3855.

[84] Q. Liu, Y.-N. Li, H.-H. Zhang, B. Chen, C.-H. Tung, L.-Z. Wu, 'Reactivity and Mechanistic Insight into Visible-Light-Induced Aerobic Cross-Dehydrogenative Coupling Reaction by Organophotocatalysts', *Chem. Eur. J.* **2012**, *18*, 620 – 627.

[85] A. S.-K. Tsang, M. H. Todd, 'Facile synthesis of vicinal diamines via oxidation of *N*-phenyltetrahydroisoquinolines with DDQ', *Tetrahedron Lett.* **2009**, *50*, 1199 – 1202.

[86] T. Nobuta, N. Tada, A. Fujiya, A. Kariya, T. Miura, A. Itoh, 'Molecular Iodine Catalyzed Cross-Dehydrogenative Coupling Reaction between Two sp^3 C–H Bonds Using Hydrogen Peroxide', *Org. Lett.* **2013**, *15*, 574 – 577.

[87] H. Ueda, K. Yoshida, H. Tokuyama, 'Acetic Acid Promoted Metal-Free Aerobic Carbon–Carbon Bond Forming Reactions at α-Position of Tertiary Amines', *Org. Lett.* **2014**, *16*, 4194 – 4197.

[88] D. Kundu, R. K. Debnath, A. Majee, A. Hajra, 'Zwitterionic-type molten salt-catalyzed *syn*-selective aza-Henry reaction: solvent-free one-pot synthesis of β-nitroamines', *Tetrahedron Lett.* **2009**, *50*, 6998 – 7000.

[89] A. Tanoue, W.-J. Yoo, S. Kobayashi, 'Sulfuryl Chloride as an Efficient Initiator for the Metal-Free Aerobic Cross-Dehydrogenative Coupling Reaction of Tertiary Amines', *Org. Lett.* **2014**, *16*, 2346 – 2349.

[90] Z. Li, C.-J. Li, 'Highly Efficient Copper-Catalyzed Nitro-Mannich Type Reaction: Cross-Dehydrogenative-Coupling between sp^3 C–H Bond and sp^3 C–H Bond', *J. Am. Chem. Soc.* **2005**, *127*, 3672 – 3673.

[91] H. Yokoi, S. Hiroto, H. Shinokubo, 'Reversible σ-Bond Formation in Bowl-Shaped π-Radical Cations: The Effects of Curved and Planar Structures', *J. Am. Chem. Soc.* **2018**, *140*, 4649 – 4655.

[92] J. L. Clark, J. E. Hill, I. D. Rettig, J. J. Beres, R. Ziniuk, T. Y. Ohulchanskyy, T. M. McCormick, M. R. Detty, 'Importance of Singlet Oxygen in Photocatalytic Reactions of 2-Aryl-1,2,3,4-tetrahydroisoquinolines Using Chalcogenoroxamine Photocatalysts', *Organometallics* **2019**, *38*, 2431 – 2442.

[93] L. Zhang, W. Wang, A. Wang, Y. Cui, X. Yang, Y. Huang, X. Liu, W. Liu, J.-Y. Son, H. Oji, T. Zhang, 'Aerobic oxidative coupling of alcohols and amines over Au – Pd/resin in water: Au/Pd molar ratios switch the reaction pathways to amides or imines', *Green Chem.* **2013**, *15*, 2680 – 2684.

[94] C. Hansch, A. Leo, R. Taft, 'A Survey of Hammett Substituent Constants and Resonance and Field Parameters', *Chem. Rev.* **1991**, *91*, 165 – 195.

[95] E. Boess, D. Sureshkumar, A. Sud, C. Wirtz, C. Fares, M. Klussmann, 'Mechanistic Studies on a Cu – Catalyzed Aerobic Oxidative Coupling Reaction with *N*-Phenyl Tetrahydroisoquinoline: Structure of Intermediates and the Role of Methanol As a Solvent', *J. Am. Chem. Soc.* **2011**, *133*, 8106 – 8109.

[96] E. Boess, C. Schmitz, M. Klussmann, 'A Comparative Mechanistic Study of Cu – Catalyzed Oxidative Coupling Reactions with *N*-Phenyltetrahydroisoquinoline', *J. Am. Chem. Soc.* **2012**, *134*, 5317 – 5325.

[97] M. O. Ratnikov, M. P. Doyle, 'Mechanistic Investigation of Oxidative Mannich Reaction with *tert*-Butyl Hydroperoxide. The Role of Transition Metal Salt', *J. Am. Chem. Soc.* **2013**, *135*, 1549 – 1557.

[98] J. Zhang, B. Tiwari, C. Xing, X. Chen, Y. R. Chi, 'Enantioselective Oxidative Cross-Dehydrogenative Coupling of Tertiary Amines to Aldehydes', *Angew. Chem. Int. Ed.* **2012**, *51*, 3649 – 3652.

[99] L. Huang, J. Zhao, 'C_{60}-Bodipy dyad triplet photosensitizers as organic photocatalysts for photocatalytic tandem oxidation/[3 + 2] cycloaddition reactions to prepare pyrrolo[2,1-*a*]isoquinoline', *Chem. Commun.* **2013**, *49*, 3751 – 3753.

[100] Q. Xia, H. Tian, J. Dong, Y. Qu, L. Li, H. Song, Y. Liu, Q. Wang, '*N*-Arylamines Coupled with Aldehydes, Ketones, and Imines by Means of Photocatalytic Proton-Coupled Electron Transfer', *Chem. Eur. J.* **2018**, *24*, 9269 – 9273.

[101] X. Meng, Y. Wang, B. Chen, G. Chen, Z. Jing, P. Zhao, 'OMS-2/H_2O_2/Dimethyl Carbonate: An Environmentally-Friendly Heterogeneous Catalytic System for the Oxidative Synthesis of Benzoxazoles at Room Temperature', *Org. Process Res. Dev.* **2017**, *21*, 2018 – 2024.

[102] M. Cherest, X. Lusinchi, 'Reaction des nitrones avec les chlorures d'acides: action de chlorures d'aryl-sulfonyles et du chlorure de benzoyle sur des n-oxy (aryl-1 dihydro-3,4 isoquinoleines). Formation d'une isoquinoleine, d'un isocarbostyryle ou d'une indoline selon les conditions', *Tetrahedron* **1982**, *38*, 3471 – 3478.

[103] H. E. Ho, Y. Ishikawa, N. Asao, Y. Yamamoto, T. Jin, 'Highly efficient heterogeneous aerobic cross-dehydrogenative coupling *via* C–H functionalization of tertiary amines using a nanoporous gold skeleton catalyst', *Chem. Commun.* **2015**, *51*, 12764 – 12767.

Received September 21, 2020
Accepted November 10, 2020

